Materials Science and Engineering C 68 (2016) 299–307

Contents lists available at ScienceDirect

Materials Science and Engineering C

journal homepage: www.elsevier.com/locate/msec

Poloxamer 407/188 binary thermosensitive hydrogels as delivery systems for infiltrative local anesthesia: Physico-chemical characterization and pharmacological evaluation

Alessandra C.S. Akkari [a], Juliana Z. Boava Papini [b], Gabriella K. Garcia [a], Margareth K.K. Dias Franco [c], Leide P. Cavalcanti [d], Antonio Gasperini [e], Melissa Inger Alkschbirs [e], Fabiano Yokaichyia [f], Eneida de Paula [g], Giovana R. Tófoli [h], Daniele R. de Araujo [a,*]

[a] Human and Natural Sciences Center, ABC Federal University, Santo André, SP, Brazil
[b] São Francisco University, Bragança Paulista, São Paulo, Brazil
[c] Nuclear and Energy Research Institute, São Paulo, SP, Brazil
[d] School of Chemical Engineering, University of Campinas, SP, Brazil
[e] Brazilian Synchrotron Light Laboratory, Campinas, SP, Brazil
[f] Department Quantum Phenomena in Novel Materials Helmholtz-Zentrum Berlin für Materialien und Energie GmbH, Berlin, Germany
[g] Department of Biochemistry, Institute of Biology, State University of Campinas, Campinas, SP, Brazil
[h] Faculty of Dentistry São Leopoldo Mandic, Campinas, São Paulo, Brazil

ARTICLE INFO

Article history:
Received 17 January 2016
Received in revised form 6 April 2016
Accepted 20 May 2016
Available online 20 May 2016

Keywords:
Poloxamer
Micelle
Hydrogel
Ropivacaine
Local anesthesia

ABSTRACT

In this study, we reported the development and the physico-chemical characterization of poloxamer 407 (PL407) and poloxamer 188 (PL188) binary systems as hydrogels for delivering ropivacaine (RVC), as drug model, and investigate their use in infiltrative local anesthesia for applications on the treatment of post-operative pain. We studied drug-micelle interaction and micellization process by light scattering and differential scanning calorimetry (DSC), the sol-gel transition and hydrogel supramolecular structure by small-angle-X-ray scattering (SAXS) and morphological evaluation by Scanning Electron Microscopy (SEM). In addition, we have presented the investigation of drug release mechanisms, *in vitro*/*in vivo* toxic and analgesic effects. Micellar dimensions evaluation showed the formation of PL407-PL188 mixed micelles and the drug incorporation, as well as the DSC studies showed increased enthalpy values for micelles formation after addition of PL 188 and RVC, indicating changes on self-assembly and the mixed micelles formation evoked by drug incorporation. SAXS studies revealed that the phase organization in hexagonal structure was not affected by RVC insertion into the hydrogels, maintaining their supramolecular structure. SEM analysis showed similar patterns after RVC addition. The RVC release followed the Higuchi model, modulated by the PL final concentration and the insertion of PL 188 into the system. Furthermore, the association PL407-PL188 induced lower *in vitro* cytotoxic effects, increased the duration of analgesia, in a single-dose model study, without evoking *in vivo* inflammation signs after local injection.

1. Introduction

Ropivacaine (RVC) is an amino-amide local anesthetic (LA) widely used in surgical procedures. Its clinical efficacy has been studied after regional anesthesia, presenting moderate time onset and considerable differentiation between the sensory and motor block, being an interesting alternative for epidural administration, infiltrative anesthesia and postoperative pain relief. One of the main advantages of RVC is the less toxicity to the central nervous and cardiovascular systems compared to bupivacaine, a well-known amino-amide local anesthetic, especially regarding to arrhythmogenic capacity, changes in heart function and occurrence of methemoglobinemia [1,2]. Numerous approaches have been used to extend the anesthetic effect and/or reduce the local and systemic toxicity evoked by LA molecules, such as the organic synthesis or enantioseparation of other LA molecules, control of the pH, association with analgesic drugs, as opioid, and also the development of drug-delivery systems [3,4]. Unfortunately, LAs are often associated with short duration of action, local and systemic toxicity.

Different drug-delivery systems has been developed for RVC, such as multivesicular [5] or unilamellar liposomes [6], PLGA microspheres [7,8]

* Corresponding author at: Centro de Ciências Naturais e Humanas, Universidade Federal do ABC, UFABC. Rua Santa Adélia, 166. Bairro Bangú. Bloco A, Torre 3, Sala 623-3, CEP 090210-580. Santo André, SP, Brasil.
E-mail addresses: daniele.araujo@ufabc.edu.br, draraujo2008@gmail.com (D.R. de Araujo).

http://dx.doi.org/10.1016/j.msec.2016.05.088
0928-4931/

and cyclodextrin complexes [9,10]. Since, the desirable features for an ideal LA are low systemic toxic potential, long duration of action and selectivity for the sensory block compared to the block motor [11], some of those systems have been achieved this goal. In this context, the development of hydrogels has been pointing them as biocompatible alternatives to avoid the rapid clearance of the drug and to extend the duration of anesthesia.

Poloxamers (PL), co-polymers composed of polyethylene oxide (PEO) and polypropylene oxide (PPO) units, have been investigated as drug-delivery systems, showing promising results concerned to the improvement of biopharmaceutics, pharmacodynamics and pharmacokinetics properties of the incorporated drugs. One of the main advantages of the PL is their capability of forming gels close to the body temperature, due to their self-assembly in micelles. In response to the temperature and concentration, the PPO hydrophobic units are dehydrated and aggregate, while the PEO hydrophilic units remain hydrated, forming the micellar core and corona, respectively. Subsequently, these micelles are self-assembled in ordered cubic or hexagonal phases, producing the thermoreversible hydrogels [12,13].

Previous studies reported the use of PL-based hydrogels for *in situ* delivery of LA molecules [14–19]. However, none of those studies have reported the relationships among physico-chemical characterization, the binary hydrogels supramolecular structure and their influence on biopharmaceutical parameters (such as release kinetics) and *in vitro*/*in vivo* toxicity. Additionally, those studies have not employed RVC for the development of a PL-based hydrogel. Then, in this work we developed hydrogels composed of PL 407 (PEO_{100}-PPO_{70}-PEO_{100}) as single or forming binary system with PL 188 (PEO_{76}-PPO_{29}-PEO_{76}). In this context, we studied the drug-micelle and micellization process interaction by light scattering and differential scanning calorimetry (DSC), the sol-gel transition and hydrogel supramolecular structure by small-angle-X-ray scattering (SAXS), the release profiles and, finally, the cytotoxic and pharmacological effects, looking forward their application for the treatment of post-operative pain.

2. Materials and methods

2.1. Materials

Poloxamer 407 (MW 12600 Da, PL407) and poloxamer 188 (MW 5800 Da, PL188) was purchased from Sigma Chem. Comp. (St. Louis, MO, USA). Ropivacaine hydrochloride (attested purity of 98.5%) was donated by Cristália Prod. Quím. Farm. Ltda (Itapira, SP, Brazil). Salts and other reagents were of analytical grade.

2.2. Physico-chemical characterization

2.2.1. Micelles and hydrogels preparation

For micellar solutions preparation, PL solutions (5% m/v, in water) containing PL 407 alone or in binary systems with PL 188 (in the presence or absence of drug) were filtered using a polycarbonate membrane (pore 0.22 μm). All measurements were determined at least five times for each sample. Hydrogels composed of PL 407 (PL188) at 20, 25 or 30% w/w alone or in association with poloxamer 188 (PL 188) at 5 or 10% w/w (30% PL final concentration), were dispersed in deionized water until complete dissolution and kept at 4 °C under magnetic stirring (150 rpm) [20,21]. RVC hydrochloride was dispersed into PL solutions or hydrogels at 0.5% (m/v) final concentration. The polymeric dispersions were then left at 4 °C until the use.

2.2.2. Micellar hydrodynamic diameter

The micellar hydrodynamic diameter and the size average distribution size were determined using a particle analyzer Zetasizer ZS (Malvern®, UK) at a fixed angle of 173° and temperatures of 25° and 37 °C, in order to simulate the micelles behavior at room and physiological temperature. After prepared and filtered (polycarbonate membrane with pore 0.22 μm), 5 wt% PL 407 solutions were analyzed in the presence or absence of RVC. All measurements were determined at least five times for each sample.

2.2.3. Differential scanning calorimetry (DSC) analysis

PL hydrogels (35 mg) were placed in sealed aluminum pans and submitted to three successive thermal cycles of heating-cooling from 0 °C to 50 °C at a rate of 5 °C/min, using a TA Instruments (USA) Q-200 DSC apparatus. An empty pan was used as reference. All analyzes were performed in triplicate and thermograms represented by heat flux ($kJ \cdot mol^{-1}$) *versus* temperature (°C).

2.2.4. Rheological analysis

The rheological analysis of the hydrogels samples were carried out using a Kinexus rotational rheometer (Malvern Instruments Ltd., England, UK). Measurements were performed at a temperature range from 10 to 50 °C using a cone-plate geometry (40 mm of diameter size), a sample volume of 1 mL, a gap between the plates of 1 mm, frequency of 1 Hz and shear stress of 2 Pa. The oscillatory measurements were used to determine parameters related to the elastic modulus (G'), the viscous modulus (G'') and viscosity (η). rSpace for Kinexus® software was used to analyze the data.

2.2.5. Small-angle X-ray scattering (SAXS)

The SAXS measurements were carried out at SAXS 1 beamline (National Laboratory of Synchrotron Light-LNLS, Campinas, SP, Brazil), using an incident beam energy of 8.3 keV (lambda = 1.488 Å) with distance between sample and detector 1007 mm (MarCCD detector with a diameter of 165 mm) and measuring range (brand measuring range) from 0:13 to 3:34 nm^{-1}. Measurements were performed at two different temperatures (25 and 37 °C). The measured scattered intensity was displayed as a function of the scattering vector modulus $q = 4\pi\sin(\theta)/\lambda$, where 2θ is the scattering angle and λ is the radiation wavelength. The typical q range was from 0.075 to 0.23 $Å^{-1}$.

2.2.6. Scanning Electron Microscopy (SEM)

Morphological features of RVC, PL-based formulations were analyzed by Scanning Electron Microscopy (SEM). For samples preparation, PL hydrogels were placed in a glass slide, forming a thin film, incubated at 40 °C for 24 h and analyzed by a scanning electron microscope with a magnification of 250 times and accelerating voltage of 1 kV.

2.3. Drug loading and in vitro release assays

For drug loading determination, samples of the hydrogel (1 g) were solubilized in 100 mL of pH 7.4 20 mM Hepes buffer plus 154 mM NaCl and stored for 48 h. Samples were then centrifuged (5000 rpm for 20 min) and 1 mL of the supernatant was analyzed by UV-VIS spectrophotometry. The percentage drug loading (DL, %) was determined according to the Eq. (1):

$$DL\ (\%) = (\text{mass of drug in hydrogel samples}/\text{mass of samples}) \times 100 \quad (1)$$

In vitro release assays were carried out in a membrane diffusion model in vertical Franz-type cells with 1.76 cm^2 permeation area (Automatized Microette Plus® Hanson Research, CA, USA), with artificial membrane (cellulose acetate sheets, MWCO 1000 Da., Spectrum Lab) as barrier. The donnor compartment was filled with 1 g of the hydrogels containing RVC (0.5% or 5 $mg \cdot mL^{-1}$), while the receptor compartment with 5 mM Hepes with 154 mM NaCl buffer, pH 7.4, at 37 °C under constant magnetic stirring (350 rpm). At predetermined time points, aliquots from receptor compartment were withdrawn (1 mL) and analyzed by UV-VIS spectrophotometry (263 nm, $y = -0.00337 + 0.44401\times$, $R^2 = 0.99974$, LQ = 0.0078 $mg \cdot mL^{-1}$; LD = 0.02406 $mg \cdot mL^{-1}$, analytical curve previously obtained). Data

were expressed as percentage of RVC cumulative release for each sample (n = 6).

Then, the *in vitro* release data were analyzed according to the mathematic models:

$$Q_t = Q_0 + K_{0\cdot t} \quad (2)$$

where, Q_t is the cumulative amount of drug released at time t, Q_0 is the initial amount of drug, K_0 the zero-order release constant, and t is time;

$$Q_t = K_{H\cdot t}^{1/2} \quad (3)$$

K_H is the release coefficient, following the Fick's law and Q_t is the amount of drug released;

$$Q_0^{1/3} - Q_t^{1/3} = K_{HC\cdot t} \quad (4)$$

Q_0 is the initial amount of drug, Qt is the cumulative amount of drug released, K_{HC} is the release constant and t is the time.

2.4. In vitro citotoxicity assays

Cell viability tests were performed using *Balb/c* fibroblasts (3T3 cells) cultured in DMEM supplemented with 10% fetal bovine serum (pH 7.2–7.4, humidified atmosphere at 37 °C and 5% CO_2), seeded in 96-wells tissue culture plates and cultured for 48 h (2.10^4 cells/well). Cells were incubated for 3 h with RVC, PL 407 and the system PL407-RVC. Drug concentrations tested were 1; 2 and 4 mM (0.312; 0.625 and 1.25 mg/mL, respectively) and PL 407 or PL 407-PL188 control groups (RVC-free) were added into the cell cultures at the same volume for the systems containing RVC. The drug:poloxamer (RVC:PL) proportion was maintained at 1:10 (mg/mL) for all formulations into the cell culture wells, at final volume of 0.1 mL. The number of viable cells was determined by measuring the MTT converted to formazan. The produced formazan crystals were solubilized in a 1 N HCl-isopropyl alcohol mixture (1:24 v/v). After that, the dye-containing solution was removed and the sample absorbance determined at 570 nm [22].

2.5. In vivo local toxicity and pharmacological evaluation

Male adults Wistar rats (300–350 g) were obtained from São Francisco University (Biotério Central, São Francisco University-USF, Bragança Paulista, SP, Brazil). Experimental protocol was approved by the USF Institutional Animal Care and Use Committee, which follows the recommendations of the Guide for the Care and Use of Laboratory Animals (protocol number 0011209).

The paw edema test was performed as model to assess the *in vivo* local toxicity and the capability of PL407, PL 407-PL188, RVC and PL 407-RVC or PL 407-PL188-RVC for inducing inflammation after intraplantar injection. This animal model is based on carrageenan mechanism of action, a mucopolysacharide from Irish Sea mosses (*Chondrus*), which stimulates an inflammatory process without systemic effects. For this test, carrageenan solution (1%) was used as positive control and 154 mM NaCl solution as negative control. Before the test, animals were anesthetized with 40 $mg \cdot kg^{-1}$ of sodium thiopental (intraperitoneal route) and the paw limit evidenced. Then, the paw baseline volume was measured for each animal and, after that, test and control solutions were administered by intraplantar injections (0.1 mL). At regular intervals, 60, 120, and 180 min after injection the rat paw volume was measured with a plethysmometer (Ugo-Basile, Varese, Italy) and expressed in milliliters, as the difference between the baseline and the injected paw volume [10,23–24].

The analgesic effects were evaluated using the tail-flick test, after animals treatment with 0.5% RVC or hydrogels at the same drug concentration. For the baseline measurement (normal response to the noxious stimulus) the animal was placed in a horizontal acrylic restraint and fixed on an analgesimeter with the tail region (5 cm from its tip) exposed to heat from a projector lamp (55 ± 1 °C. 150 W). The time for normal response (in seconds) was recorded by a control switch and a timer simultaneously activated when the rat tail flicks. The formulations (RVC in water or hydrogels) were injected on the tail base (0.1 mL total, where 0.05 mL for each tail side). After 1 min, the tail was exposed to the heat and the interval between switching on the light and flick of the tail was recorded (latency time). A 30-s cut-off time was used to avoid thermal injury. The evaluation was started 10 min after application of the formulations and at the same interval until the baseline values. All experiments were carried out by the same observer. Data were expressed as maximum percentual effect (MPE %), duration of the analgesic effect (minutes) and area under the efficacy curve (AUEC) for each experimental group.

$$MPE = (\text{latency time} - \text{baseline} / \textit{cutoff} - \text{baseline}) \times 100$$

2.6. Statistical analysis

Data were expressed mean ± S.D. and analyzed by One-way analysis of variance (One-way ANOVA) with Tukey-Kramer *post hoc* test. Graph Pad Instat (Graph Pad Software Inc., USA) or Origin 6.0 (Microcal™ Software, Inc., Northampton, MA, USA) programs were used. Statistical differences were defined as $p < 0.05$.

3. Results and discussion

3.1. Drug-micelle interaction: micellar hydrodynamic diameter and average size distribution

The drug-micelle interaction was assessed by Dynamic Light Scattering (DLS), being possible to observe the effects of the temperature, micelle composition and also the drug incorporation on micellar hydrodynamic diameter and size distribution parameters. Table 1 summarizes the results.

The micelle hydrodynamic diameter, at 25 °C, for the systems composed only of PL 407 was ~30 nm and 8.6 nm, with 87% and 12% of average size distribution, respectively. However, at 37 °C, it was observed a micellar population with reduced diameter (~25 nm with 100% of size distribution), showing a shift from bimodal to unimodal system with low polydispersity index values (from 0.246 to 0.143 at 25 °C and 37 °C). On the other hand, for binary systems PL 407/PL 188 it was observed higher values of hydrodynamic diameter (~47 to 60 nm) for both proportions and temperatures evaluated, and also high polydispersion index (~0.4), suggesting the formation of mixed micelles composed of

Table 1
Hydrodynamic diameter (nm) and average distribution (%) of PL407 isolated or associated to PL188 micelles before and after ropivacaine incorporation.

Formulations	25 °C		37 °C	
	Hydrodynamic diameter (nm)	Average distribution (%)	Hydrodynamic diameter (nm)	Average distribution (%)
PL 407	32.4 ± 0.1	87.3	25.4 ± 0.3	100
	8.6 ± 1.6	12.7		
PL 407-RVC	30.7 ± 0.4	88.5	24.8 ± 0.4	100
	6.2 ± 0.5	11.5	–	–
PL 407-PL 188	58.2 ± 0.6	86.4	56.4 ± 0.1	84.3
(2:1)[a]	6.5 ± 0.1	13.6	5.6 ± 0.2	15.6
PL 407-PL 188	60.2 ± 0.4	89.1	56.6 ± 0.6	85.2
(2:1)-RVC	5.3 ± 0.1	10.9	5.5 ± 0.1	14.8
PL 407-PL 188	47.5 ± 0.7	82.3	43.7 ± 0.5	86.9
(5:1)[b]	5.9 ± 0.7	18.7	5.1 ± 0.4	13.1
PL 407-PL 188	48.7 ± 0.2	75.4	42.7 ± 0.6	87.3
(5:1)-RVC	6.2 ± 0.3	24.6	5.4 ± 0.1	12.6

Note: PL407-PL188 ratios are expressed as % w/v, with 2:1 and 5:1 corresponding to the formulations PL407-PL188 20–10 and PL407-PL188 25–5, respectively.

copolymers with high molecular mass (PL 407 = 12.600 and PL 188 = 8400) and hydration, since PL 188 is more hydrophilic than PL 407 (with hydrophilic lipophilic balances-HLB of 29 and 22, respectively) [25].

Previous works reported the reduction on micellar dimensions for poloxamer-based delivery systems, as a function of temperature. In fact, other authors [26] have described that the micellar hydrodynamic radius was reduced at 35 °C, showing a relationship between this parameter, the dehydration of PPO units and also the viscosity of the formulation, favoring the formation of a colloidal system with homogeneous spherical micelles [27]. Also, in this work, micellar hydrodynamic diameter determination was important to observe the drug-micelle interaction, since the incorporation of RVC did not change the micellar dimensions.

3.2. Differential scanning calorimetry (DSC)

The temperatures (T_m) and enthalpy (ΔH_m°) relatively to the micellization were determined by differential scanning calorimetry (DSC). Data are presented on Table 2. In general, all formulations showed a thermoreversible behavior since transition peaks were observed in both heating and cooling cycles. Besides, it was also possible to verify the homogeneity between both copolymers, since only one transition phase was observed in the thermograms, even for the systems containing RVC.

The first analysis showed that low values of temperatures for micellization (T_m) were observed for the high copolymer concentration, considering the systems composed only of PL 407. In a different manner, T_m values for binary systems (PL 407-PL 188) were similar, even after RVC incorporation.

Formulations containing only PL 407 presented similar ΔH° values. This result was also observed for PL 407-RVC. On the other hand, for binary systems, the enthalpy of micelles formation changed after the addition of PL 188 and RVC. Despite the same copolymer total concentration, different ratios PL 407/PL 188 induced high ΔH° values, when compared to the PL 407 formulations. For example, the system PL 407-PL 188 (20:10% w/w, PL 407:PL 188 proportion 2:1) showed ΔH° value of 31.7 $kJ \cdot mol^{-1}$. However, for PL 407-PL 188-RVC the ΔH° was 39.2 $kJ \cdot mol^{-1}$. More pronounced changes were obtained for PL 407-PL 188 (25:5% w/w, PL 407:PL 188 proportion 5:1). RVC is an amino-amide local anesthetic relatively hydrophobic (with partition coefficient lipid/water of 132) [6]. Even RVC incorporation did not influence the micellar dimensions, changes were observed on self-assembly and the mixed micelles formation (as seen by the differences on enthalpy variation values) especially for the binary systems with high concentration of PL407. It is important to notice that RVC is presented as its salt form (RVC hydrocholide), which alters the tendency of micelles to "package" after the addition of a salt, due to dehydration of PPO units into the micellar core.

In this context, the association between copolymers with different HLB values induces conformational changes on micellar assembly, since PL 188 (HLB = 29) is a more hydrophilic copolymer than PL 407 (HLB = 22) the hydration of the micellar corona is increased, due to the high number of PEO units into the PL 188 monomers [25,26], explaining the low ΔH° values for the binary system PL 407-PL 188 (25–5% w/w, PL 407:PL188).

Table 2
Temperature micellization (T_m) and enthalpy variation (ΔH°_m) for PL407 isolated or in association with PL188.

Formulations	PL (% w/v)	T_m (°C)	ΔH°_m ($kJ \cdot mol^{-1}$)
PL 407	20	15.1	49.6
	25	12.8	52.4
	30	10.6	54.4
PL407-RVC	20	14.7	47.9
	25	12.4	50.8
	30	10.2	51.4
PL 407/PL188	20/10	12.8	31.7
	25/5	11.5	56.4
PL 407/PL188-RVC	20/10	12.4	39.2
	25/5	11.7	80.9

3.3. Rheological analysis

Rheological analysis was performed for all formulations considering the different compositions and the presence or absence of RVC, being possible to determine the elastic (G′) and viscous (G″) modules, viscosity (η) and the temperature where it was observed the more pronounced viscosity variation, being considered as the sol-gel temperature (Tsol-gel). Fig. 1 shows representative rheograms with variations in G′ and G″ *versus* temperature range from 0 to 50 °C. All results for other hydrogels formulations are presented at Table 3.

In general, were observed higher G′ values in relation to G″ for most of formulations, even after RVC incorporation, revealing a viscoelastic behavior for the different formulations, since the G′ values 2–40 times higher than those observed for G″. It is important to highlight that this behavior is temperature dependent, as observed for the more pronounced viscosity values at 37 °C, in relation to 25 °C. However, PL407-PL188 20–10% binary hydrogel presented lower G′ and viscosity values when compared to the formulations composed of isolated PL407 (20, 25 or 30%) or at 25–5% PL407-PL188, showing that high concentrations of PL188 changed the rheological parameters.

The results obtained here are in agreement with other studies, since for an injectable hydrogel as depot formulation the elastic modulus should predominate over the viscous modulus, making them injectable (liquid form) at low temperatures and hydrogels at

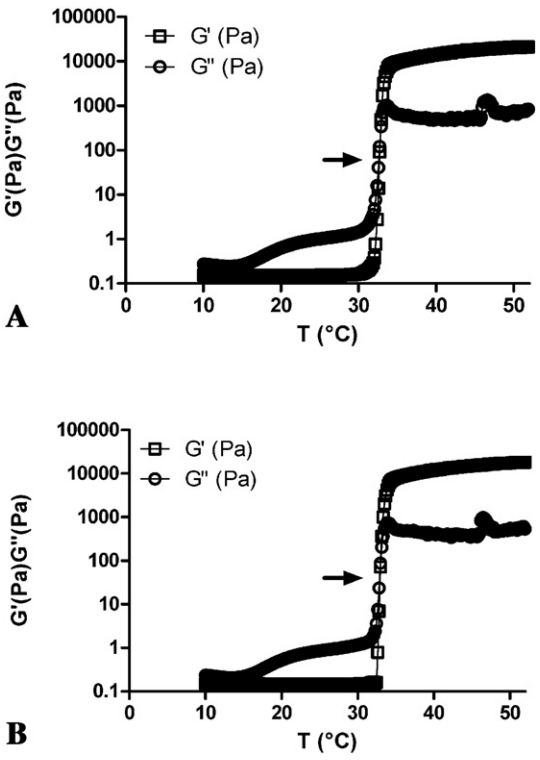

Fig. 1. Rheograms for hydrogels composed of PL407-PL188 (25–5% w/w) in the absence (A) or presence of RVC (B). The arrows indicate the sol-gel transition temperature ($T_{sol\text{-}gel}$).

Table 3
Rheological analysis presenting the elastic (G′) and viscous modules (G″) at sol-gel transition temperature, viscosity (η, at 25 and 37 °C) and sol-gel transition temperature (T sol-gel) for PL407 or PL407-PL188 hydrogels.

Formulations	G′ (Pa)	G″ (Pa)	G′/G″	η (mPa·s)		T gel (°C)
				25 °C	37 °C	
PL407 20%	10,160	475.5	21.4	111.2	1.6×10^6	27.1
PL407 20%-RVC	10,120	480.2	21.1	117.7	1.7×10^6	27.6
PL407-25 %	19,640	489.2	40.1	2.1×10^6	3.1×10^6	22.7
PL407 25% - RVC	13,454	362.2	37.1	1.5×10^6	2.3×10^6	23.0
PL407-30%	62,980	25310	2.5	3.3×10^6	4.2×10^6	19.4
PL407-30%-RVC	4124	810	5.1	2.9×10^6	3.6×10^6	20.2
PL407-PL188 25-5%	1400	400	3.5	1.6×10^4	1.8×10^6	32.6
PL407-PL188 25-5%-RVC	362.1	202.8	1.8	1.4×10^5	1.5×10^6	33.1
PL407-PL188 20-10%	0.18	3.2	0.05	61.5	70.2	>50
PL407-PL188 20-10%-RVC	0.19	3.1	0.06	61.6	70.2	>50

physiological temperature. Those features can modulate biopharmaceutical properties such as dissolution and release rates [16,17]. In this context, we observe that the formulation PL407-PL188 25–5% presented the $T_{sol\text{-}gel}$ close to the physiological temperature being adequate for the purpose of an injectable hydrogel.

3.4. Hydrogels structural characterization: SAXS

The scattering patterns are shown in fig. 2. At 25 °C all systems presented lamellar structure with spacing $D = 2\pi/q^* \sim 17.6$ nm, for PL 407 20% and ~19 nm for PL 407 25% associated to PL 188 at 5%. However, considering the temperature at 37 °C, exhibited a phase organization in hexagonal structure, as can be seen from the peak positions at q*, 31/2q*, 2q* and 71/2q*, with $q^* \sim 0.352\ nm^{-1}$ for PL 407 20% and $q^* \sim 0.349\ nm^{-1}$ for PL 407 25%/PL 188 5%, corresponding to a distance of roughly 18 nm between micellar centers in both systems.

In addition, the inclusion of RVC did not affect the supramolecular structure of the systems, since the position and intensity of the peaks were not changed by its presence. For the smaller *q* region observed in the patterns, the scattering intensity presented a discrete change with temperature and incorporation of RVC. This result might indicate that RVC interfere in the macrostructure of the system, since the hexagonal phase organization can facilitate the drug incorporation into the intermicellar spaces. Our results are in agreement with previous study that reported the formation of hexagonal phase for PL-based binary systems, indicating that the gelation process is due to the ordered assembly of micelles in a dependent manner of the incorporation of PL with intermediate or low hydrophilic lipophilic balance values [28,29].

3.5. Morphological evaluation: SEM analysis

Fig. 3A illustrates the arrangement of typical RVC crystals with morphology elongated, sharp and a cubic-rectangular shape. On the other hand, all PL-based systems presented a layered morphology, as particularly observed for PL407 (25%) (Fig. 3B), PL407-RVC (25%) (Fig. 3C), PL407-PL188 (25–5%) (Fig. 3D) and PL407-PL188-RVC (25–5%) (Fig. 3E), where it was not found similar structures than that observed for RVC crystals, indicating that the drug was incorporated into the hydrogels, in agreement with patterns observed in a previous study [30].

3.6. Drug loading and in vitro release studies

Drug loading (DL) experiments were performed for all hydrogels formulations using a membraneless model in order to simulate a condition of total dissolution of the hydrogels. In general, the DL was ~96% (after 48 h), showing the homogeneity of the drug content into hydrogels (Table 4). Fig. 4 shows the RVC release profiles, across artificial membrane (cellulose acetate), from the different hydrogels formulations. The drug release, in solution (commercially available for injection), was progressive and the total release was reached at 8 h

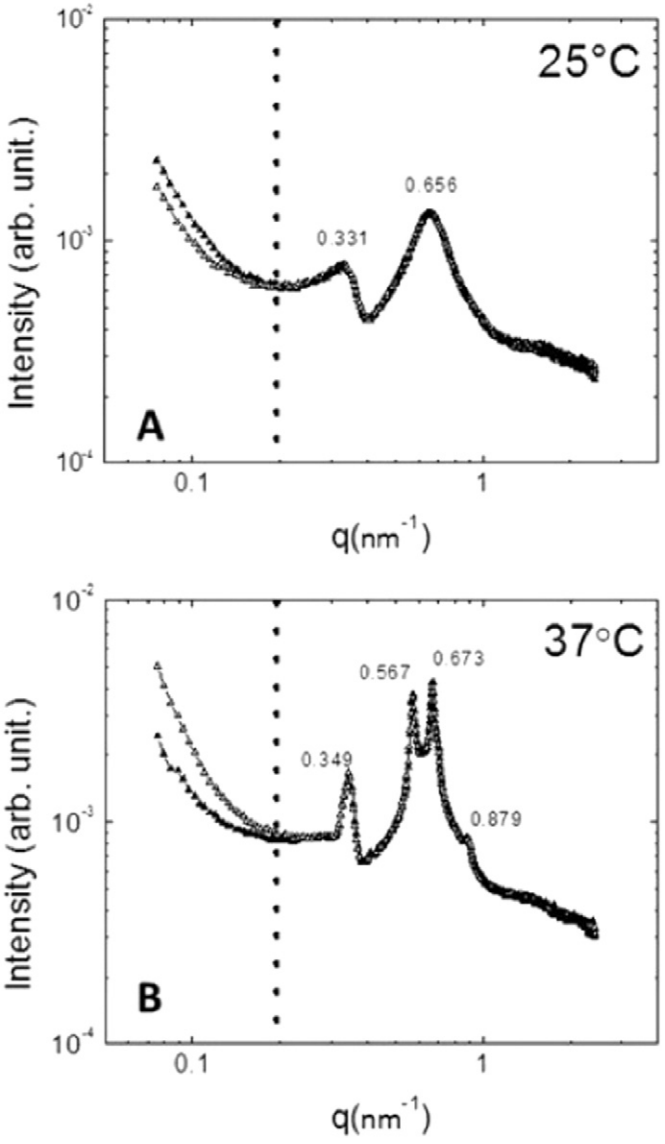

Fig. 2. SAXS profiles for the binary hydrogel PL407-PL188 at 25 °C (A) and 37 °C before and after ropivacaine (RVC) incorporation (Δ-PL407-PL188-RVC and ▲-PL407-PL188).

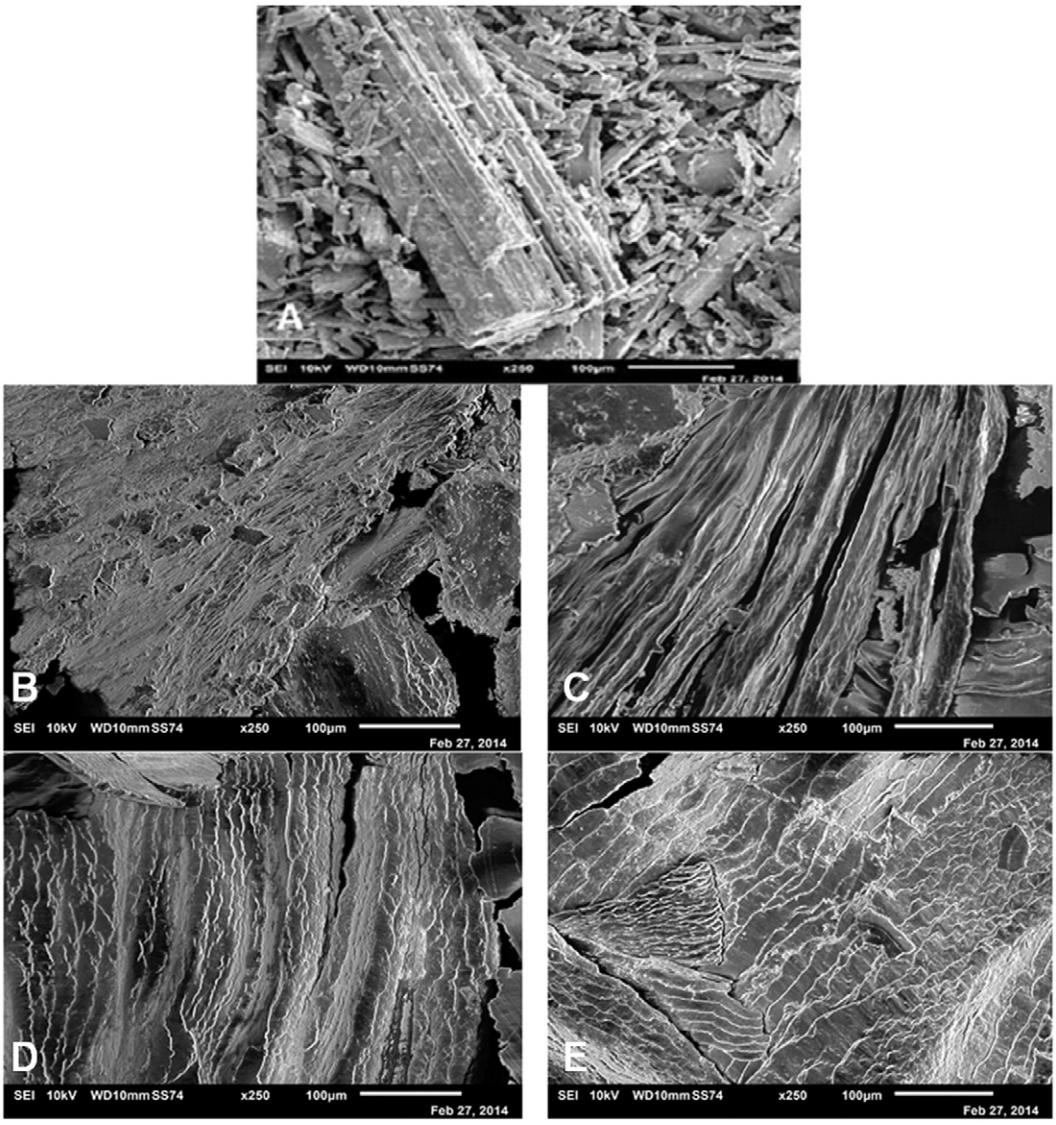

Fig. 3. Scanning Electron Microscopy obtained for ropivacaine (RVC, A), PL 407-PL188 (B) and PL407-PL188-RVC (C).

(~100% RVC released). However, the hydrogel formulations showed regular release profiles and lower RVC released percentages were observed for 25% PL 407 (75.1 ± 1.3%); 30% PL 407 (73.7 ± 2.3%); 25–5% PL 407-PL188 (83.2% ± 0.5%) and 20–10% PL407-PL188 (96.5 ± 2.1%), when compared to the drug in solution, at 24 h. The release constants (K_{rel}) were, then, calculated according to the Zero Order, Higuchi and Hixson-Crowel models.

After comparisons, statistical differences were observed for hydrogels formulation in relation to the RVC solution ($p < 0.05$), presenting higher correlation coefficient values obtained for the Higuchi model ($0.92 > R^2 > 0.96$) and indicating that the RVC release follows the Fick's law, associated to the diffusion of the drug through the hydrogels until reach the site of action.

The lower K_{rel} values were observed for 25% or 30% PL407 and its binary system 25–5% PL407-PL188, showing that the PL final concentration and also the insertion of PL 188 into the formulations were able to modulate the RVC release. Then, considering the K_{rel} values, the formulation composition and the PL407 concentration, the hydrogels

Table 4
Drug release constants, correlation coefficients and drug loading percentage obtained for PL407 isolated or in association with PL188 hydrogels.

Formulations	Zero-order		Higuchi		Hixson-Crowel		Drug loading (% at 48 h[a])
	K_0 (%.h^1)	R^2	K_H (%.h$^{-1/2}$)	R^2	K_{HC} (%.h$^{-1/3}$)	R^2	
RVC	5.2 ± 0.6	0.806	19.5 ± 0.6	0.920	27.8 ± 2.7	0.870	–
PL407–25%	3.2 ± 0.2*	0.769	14.2 ± 1.4*	0.961	19.5 ± 2.1*	0.833	96.7 ± 1.1%
PL407–30%	3.1 ± 0.5*	0.738	13.4 ± 0.8*	0.937	16.0 ± 0.5*	0.822	96.2 ± 0.4%
PL407-PL188 (25–5%)	3.5 ± 0.3*	0.737	13.5 ± 1.2*	0.941	20.3 ± 0.7*	0.818	96.2 ± 0.7%
PL407-PL188 (20–10%)	4.6 ± 0.3*	0.917	16.0 ± 0.6*	0.918	24.2 ± 0.5	0.907	96.5 ± 1.8%

Note: Data presented as mean ± S.D. (n = 6/formulation).
* $p < 0.05$: statistical difference compared to RVC solution (in water).
[a] Drug loading was determined using a membraneless model.

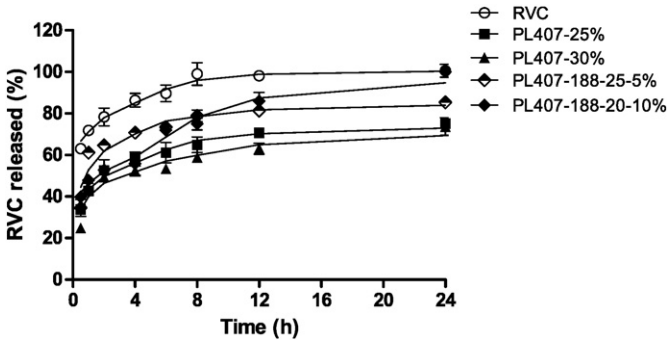

Fig. 4. Release profiles for ropivacaine (RVC) from PL 407 and PL 407-PL188 hydrogels (n = 6/formulation).

formulations RVC-PL407-PL188 (25–5%) and its similar RVC-PL407 (25%) were evaluated according to *in vitro*/*in vivo* toxicity and anesthetic effects.

The most accepted mechanism to explain the PL thermogelling phenomenon refers to the interaction between the units of the copolymer. The monomers of these copolymers, above the critical micelle concentration (CMC), are organized in micelles (when in aqueous medium) in order to minimize the free energy. As the temperature increases, the equilibrium between micelles and unimers is favored towards micellization due to dehydration of propylene oxide units, providing a structural change. The connection of the polymer network, with subsequent gel formation, is due to the micelles aggregation assuming hexagonal and/or cubic structures (depending on the type and concentration of copolymers). This phenomenon is reversible and when the temperature decreases, it occurs the hydration of the propylene oxide units and

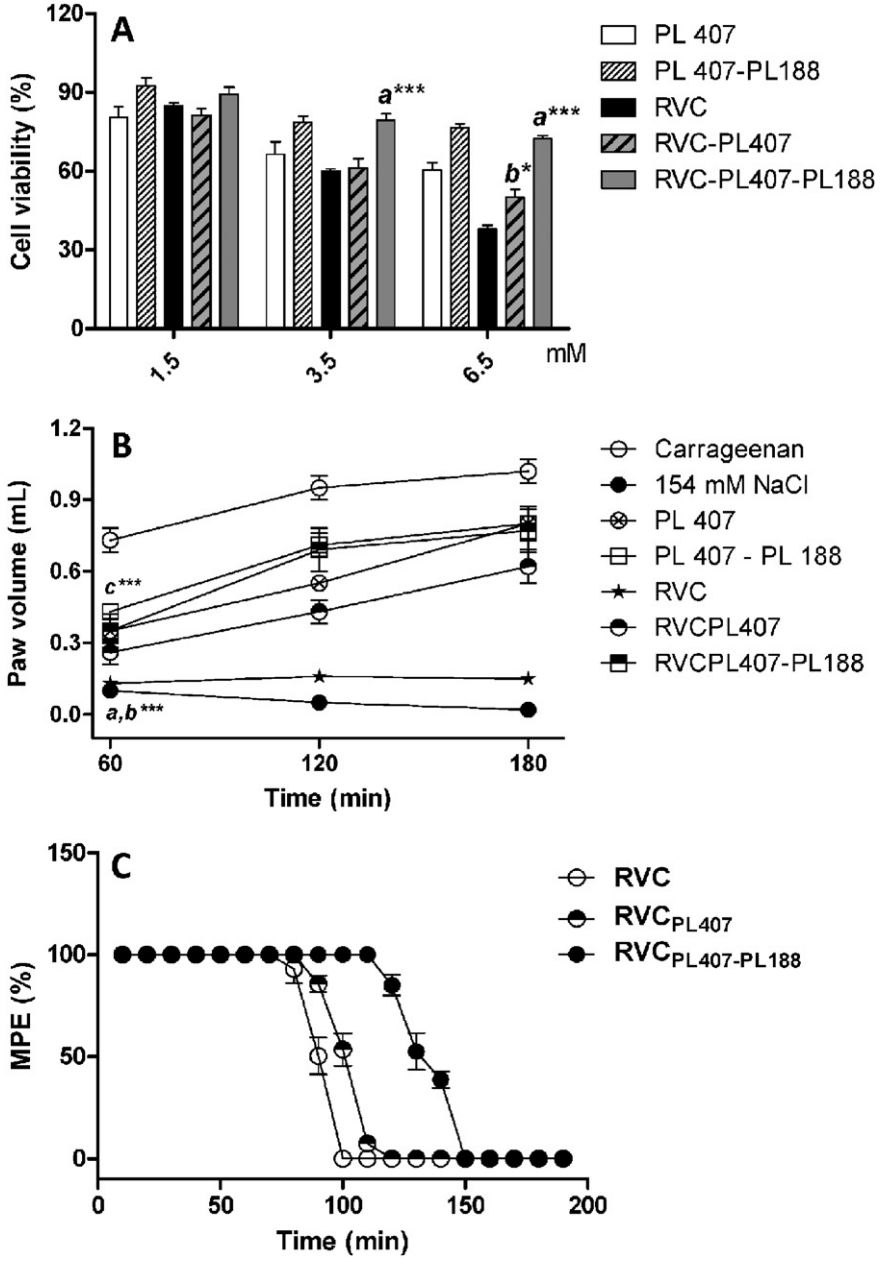

Fig. 5. Effects of PL407 or PL407-PL188 systems on 3T3-fibrolasts viability (A), paw edema (B) and tail flick test (C). Data expressed as mean ± S.D. a-PL407-RVC *vs.* RVC; b-PL407-PL188-RVC *vs.* RVC; c-PL407 or PL407-PL188 hydrogels *vs.* carrageenan group. One–way ANOVA with Tukey-Kramer post hoc test. *$p < 0.05$; *** $p < 0.001$ (n = 6–7/formulation).

the micelles self-assembly and aggregation in solution, from phase organization lamellar to hexagonal [21,31]. In this work, we have studied a binary hydrogel associating PL with different HLB values. Since PL 188 (HLB = 29) is hydrophilic compared to PL 407 (HLB = 22) the hydration of the micellar corona is increased, but the incorporation of RVC hydrochloride (as a salt drug form) reduces the hydration of the micelles, promoting their self-assembling into a gel structure [21,31,32] and showing that release rate is affected by the hydrogel composition.

3.7. Cell viability studies, in vivo local toxicity and pharmacological evaluation

Fig. 5A show the cell viability percentage after 3T3-fibroblasts cells treatment with RVC at three different concentrations (0.312; 0.625 and 1.25 mg/mL). RVC treatment reduced the cell viability percentages, determined by MTT reduction test, showing cytotoxic effects at 0.625 and 1.25 mg/mL with 60 and 45% of viable cells, respectively. On the other hand, higher fibroblasts viability percentages (from 90 to 75%) were observed after cell treatment with PL407 and PL407-PL188. The association PL407-PL188 induced lower cytotoxic effects in 3T3-fibroblasts when compared to PL 407, which is in agreement with previous studies, using V79-fibroblasts and hepatocytes [33], 3T3 fibroblasts [34] and brain barrier vessels [35], as a result of more pronounced fluidizing effect in cell membranes for PL407 (HLB = 22) compared to PL188 (HLB = 29). In addition, the RVC incorporation in PL407-PL188 hydrogels reduced its cytotoxic effects, when compared to the drug ($p < 0.001$).

The pharmacological evaluation by the paw edema test showed that the treatment with free RVC did not induce rat paw edema, as previously reported for other local anesthetics, such as prilocaine [36] and mepivacaine [37], in a similar manner than that observed for the control group (0.9% NaCl). On the other hand, even considering that hydrogels evoked an increase on paw volume compared to the control or RVC group ($p < 0.001$), this effect was less pronounced when compared to carrageenan group ($p < 0.001$), indicating that hydrogels formulations did not induce possible local inflammatory effects (Fig. 5B), which is in agreement with previous study presenting histological evaluation after intramuscular injection of PL407 hydrogels [17]. The discrete increase on paw volume, observed here, can be attributed to the *in situ* gelling properties for all formulations, since were not observed inflammation signs (redness and local heating), as reported after carrageenan intraplantar injection [38,39].

Fig. 5C presents the evaluation of analgesic effects showing the time curve of percentual Maximum Possible Effect (MPE) obtained after treatment with RVC solution and incorporated into the hydrogels formulations. The binary hydrogel PL407-PL188 prolonged the analgesic effect (until ~150 min after injection) when compared to RVC solution (100 min) and RVCPL407 (110 min). In addition, the Area Under Effect Curve (AUEC) was also more pronounced after injection of RVCPL407-PL188, with $AUEC_{0-180}$ of 11,737 ± 549, against 7934 ± 247 and 8965 ± 621 for RVC and RVCPL407-PL188, respectively ($p < 0.001$).

One of the most strategies used for the treatment of acute or chronic pain is the therapy with local anesthetics. However, due to their short duration of action prolonged postoperative analgesia is not achieved [40,41]. Then, several drug delivery systems for local anesthetics have been developed, including injectable termosensitive hydrogels [41]. Different systems have been described such as those composed of PL407 plus sodium hyaluronate and bupivacaine [19,42], bupivacaine-PLGA-Chi microparticles in a PL407 hydrogel [43], a mixed hydrogel containing PL407-PL188, aminocaproic acid, povidone iodine, lidocaine and chitosan [34] and also a chitosan thermogel containing ropivacaine [44]. However, none of them considering the incorporation of RVC in PL407-PL188 binary systems. In addition, even considering that PL-based hydrogels dissolution is relatively fast (a desirable feature for local anesthetics delivery systems) it is necessary to note that those copolymers are considered nontoxic, there are no requirements of organic solvents, neither pH variations for their hydrogels preparation. Then, the results obtained here showed the influence of composition, concentration and poloxamer physico-chemical properties evoking low *in vitro* cytotoxicity and *in vivo* local tissue reactions. In addition, the incorporation of RVC into PL407-PL188 increased the analgesic effects. Even considering this is a single-dose study, is possible to obtain prolonged analgesia associated to possible reduced local injections, especially for future applications in post-operative pain relief and/or nerve blockade studies.

4. Conclusions

This study showed the development of PL407 and its binary systems PL407-PL188 for delivering RVC and its local tissue application for post-operative pain relief application. The physico-chemical characterization provided information about the drug-micelle interaction and its influence on hydrogel formation. The incorporation of RVC did not change the micellar dimensions, but evoked changes on micellar self-assembly for hydrogel formation, due to its possible incorporation into the intermicellar spaces and maintaining the system organization in hexagonal phase. In addition, the incorporation of PL188 into the hydrogels was able to modulate the RVC release kinetics and prolong its analgesic effects without evoking cytotoxicity or *in vivo* inflammation signs after local injection.

Acknowledgements

This research work was supported by Coordenação de Aperfeiçoamento de Pessoal de Nível Superior (CAPES), Fundação de Amparo à Pesquisa do Estado de São Paulo (FAPESP 2014/26200-9, 2014/14457-5) and Conselho Nacional de Desenvolvimento Científico e Tecnológico (CNPq 487619/2012-9, 309612/2013-6). We are also grateful to the Brazilian Synchrotron Light Laboratory for SAXS facilities (SAXS 1 beamline).

References

[1] J.B. Whiteside, J.A. Wildsmith, Developments in local anesthesia drugs, Br. J. Anaesth. 87 (2001) 27–35.
[2] L.E. Mather, The acute toxicity of local anesthetics, Expert Opin. Drug Metab. Toxicol. 6 (2010) 1313–1332.
[3] E.A. Shipton, New formulations of local anaesthetics-part I, Anesthesiol. Res. Pract. 2012 (2012) 546409.
[4] E.A. Shipton, New delivery systems for local anaesthetics-part 2, Anesthesiol. Res. Pract. 2012 (2012) 289373.
[5] Y. Shen, Y. Ji, S. Xu, Q. Chen, J. Tu, Multivesicular liposome formulations for the sustained delivery of ropivacaine hydrochloride: preparation, characterization, and pharmacokinetics, Drug Deliv. 18 (2011) 361–366.
[6] D.R. de Araujo, C.M. Cereda, G.B. Brunetto, V.U. Vomero, A. Pierucci, H.S. Neto, A.L. de Oliveira, L.F. Fraceto, A.F. Braga, E. de Paula, Pharmacological and local toxicity studies of a liposomal formulation for the novel local anaesthetic ropivacaine, J. Pharm. Pharmacol. 60 (2008) 1449–1457.
[7] Z. Zhou, J. Ye, L. Chen, A. Ma, F. Zou, Simultaneous determination of ropivacaine, bupivacaine and dexamethasone in biodegradable PLGA microspheres by high performance liquid chromatography, Yakugaku Zasshi 130 (2010) 1061–1068.
[8] M. Ratajczak-Enselme, J.P. Estebe, G. Dollo, F. Chevanne, D. Bec, J.M. Malinovsky, C. Ecoffey, P. Le Corre, Epidural, intrathecal and plasma pharmacokinetic study of epidural ropivacaine in PLGA-microspheres in sheep model, Eur. J. Pharm. Biopharm. 72 (2009) 54–61.
[9] D.R. de Araujo, S.S. Tsuneda, C.M. Cereda, F.D.G. Carvalho, P.S. Preté, S.A. Fernandes, F. Yokaichiya, M.K. Franco, I. Mazzaro, L.F. Fraceto, A.F.A. Braga, E. de Paula, Development and pharmacological evaluation of ropivacaine-2-hydroxypropyl-beta-cyclodextrin inclusion complex, Eur. J. Pharm. Sci. 33 (2008) 60–71.
[10] C.M. Cereda, G.R. Tofoli, L.G. Maturana, A. Pierucci, L.A. Nunes, M. Franz-Montan, A.L. de Oliveira, S. Arana, D.R. de Araujo, E. de Paula, Local neurotoxicity and myotoxicity evaluation of cyclodextrin complexes of bupivacaine and ropivacaine, Anesth. Analg. 115 (2012) 1234–1241.
[11] D.R. de Araujo, C.M. Cereda, G.B. Brunetto, L.M. Pinto, M.H. Santana, E. de Paula, Encapsulation of mepivacaine prolongs the analgesia provided by sciatic nerve blockade in mice, Can. J. Anaesth. 51 (2004) 566–572.
[12] L. Yu, J. Ding, Injectable hydrogels as unique biomedical materials, Chem. Soc. Rev. 37 (2008) 1473–1481.
[13] L. Klouda, A.G. Mikos, Thermoresponsive hydrogels in biomedical applications, Eur. J. Pharm. Biopharm. 68 (2008) 34–45.

[14] A. Paavola, P. Tarkkila, M. Xu, T. Wahlström, J. Yliruusi, P. Rosenberg, Controlled release gel of ibuprofen and lidocaine in epidural use-analgesia and systemic absorption in pigs, Pharm. Res. 15 (1998) 482–487.
[15] A. Paavola, J. Yliruusi, P. Rosenberg, Controlled release and dura mater permeability of lidocaine and ibuprofen from injectable poloxamer-based gels, J. Control. Release 52 (1998) 169–178.
[16] E.J. Ricci, M.V. Bentley, M. Farah, R.E. Bretas, J.M. Marchetti, Rheological characterization of poloxamer 407 lidocaine hydrochloride gels, Eur. J. Pharm. Sci. 17 (2002) 161–167.
[17] E.J. Ricci, D.M.A. Lunardi, J.M. Nanclares, J.M. Marchetti, Sustained release of lidocaine from poloxamer 407 gels, Int. J. Pharm. 288 (2005) 235–244.
[18] P.C. Chen, D.S. Kohane, Y.J. Park, R.H. Bartlett, R. Langer, V.C. Yang, Injectable microparticle-gel system for prolonged and localized lidocaine release, II. In vivo anesthetic effects, J. Biomed. Mater. Res. A. 70 (2004) 459–466.
[19] J.W. Lee, T.H. Lim, J.B. Park, Intradiscal drug delivery system for the treatment of low back pain, J. Biomed. Mater. Res. A 92 (2010) 378–385.
[20] I.R. Schmolka, Artificial skin. I. Preparation and properties of pluronic F-127 gels for treatment of burns, J. Biomed. Mater. Res. 6 (1972) 571–582.
[21] P.K. Sharma, M.J. Reilly, S.K. Bhatia, N. Sakhitab, J.D. Archambault, S.R. Bhatia, Effect of pharmaceuticals on thermoreversible gelation of PEO-PPO-PEO copolymers, Colloids Surf. B: Biointerfaces 63 (2008) 229–235.
[22] F. Denizot, R. Lang, Rapid colorimetric assay for cell growth and survival. Modifications to the tetrazolium dye procedure giving improved sensitivity and reliability, J. Immunol. Methods 89 (1986) 271–277.
[23] E.S. Fernandes, G.F. Passos, M.M. Campos, J.G. Araujo, J.L. Pesquero, M.C. Avelllar, M.M. Teixeira, J.B. Calixto, Mechanisms underlying the modulatory action of platelet activating factor (PAF) on the upregulation of kinin B1 receptors in the rat paw, Br. J. Pharmacol. 139 (2003) 973–981.
[24] S.P. Duhgaonkar, S.K. Tandan, A.S. Bhat, S.H. Jadhav, D. Kumar, Synergistic anti-inflammatory interaction between meloxicam and aminoguanidine hydrochloride in carrageenan-induced acute inflammation in rats, Life Sci. 78 (2006) 1044–1048.
[25] A.V. Kabanov, E.V. Batrakova, V.Y. Alakov, Evolution of drug delivery concept from inert nanocarriers to biological response modifiers, J. Control. Release 82 (2002) 189–212.
[26] L.C.P. Trong, M. Djabourov, A. Ponton, Mechanisms of Micellization and rheology of PEO-PPO-PEO triblock copolymers with various architectures, J. Colloid Interface Sci. 328 (2008) 278–287.
[27] Y.L. Su, J. Wang, H.Z. Liu, FTIR spectroscopic study on effects of temperature and polymer composition on the structural properties of PEO-PPO-PEO block copolymer micelles, Langmuir 18 (2002) 5370–5374.
[28] F. Artzner, S. Geiger, A. Olivier, C. Allais, S. Finet, F. Agnely, Interactions between poloxamers in aqueous solutions: micellization and gelation studied by differential scanning calorimetry, small angle X-ray scattering, and rheology, Langmuir 23 (2007) 5085–5092.
[29] A. Oshiro, D.C. da Silva, J.C. de Mello, V.W. de Moraes, L.P. Cavalcanti, M.K. Franco, M.I. Alkschbirs, L.F. Fraceto, F. Yokaichiya, T. Rodrigues, D.R. de Araujo, Pluronics F-127/L-81 binary hydrogels as drug-delivery systems: influence of physicochemical aspects on release kinetics and cytotoxicity, Langmuir 30 (2014) 13689–13698.
[30] A.C. Santos Akkari, E.V. Ramos Campos, A.F. Keppler, L.F. Fraceto, E. de Paula, G.R. Tofoli, D.R. de Araujo, Budesonide-hydroxypropyl-β-cyclodextrin inclusion complex in binary poloxamer 407/403 system for ulcerative colitis treatment: a physicochemical study from micelles to hydrogels, Colloids Surf. B: Biointerfaces 138 (2016) 138–147.
[31] T. Ur-Rehman, S. Tavellin, G. Grobner, Effect of DMSO on micellization, gelation and drug release profile of Poloxamer 407, Int. J. Pharm. 394 (2010) 92–98.
[32] N.M.P.S. Ricardo, M.E.N. Pinho, Z. Yang, D. Atwood, C. Booth, Controlling the gelation of aqueous micellar solutions of ethylene-oxide-based block copoly(oxyalkylene)s, Int. J. Pharm. 300 (2005) 22–31.
[33] A.C.M. dos Santos, A.C.S. Akkari, I.R. Ferreira, C.R. Maruyama, M. Pascoli, V.A. Guilherme, E. de Paula, L.F. Fraceto, R. de Lima, P.S. Melo, D.R. de Araujo, Poloxamer-based binary hydrogels for delivering tramadol hydrochloride: sol-gel transition studies, dissolution-release kinetics, in vitro toxicity, and pharmacological evaluation, Int. J. Nanomedicine 10 (2015) 2391–2401.
[34] L. Du, L. Tong, Y. Jin, J. Jia, Y. Liu, C. Su, S. Yu, X. Li, A multifunctional in situ-forming hydrogel for wound healing, Wound Repair Regen. 20 (2012) 904–910.
[35] E.V. Batrakova, S. Li, V.Y. Alakhov, W.F. Elmquist, D.W. Miller, A.V. Kabanov, Sensitization of cells overexpressing multidrug-resistant proteins by Pluronic P85, Pharm. Res. 10 (2003) 1581–1590.
[36] C.M. Cereda, G.R. Tofoli, R.B. de Brito Junior, M.B. de Jesus, L.F. Fraceto, F.C. Groppo, D.R. de Araujo, E. de Paula, Stability and local toxicity evaluation of a liposomal prilocaine formulation, J. Liposome. Res. 18 (2008) 329–339.
[37] G.R. Tofoli, C.M. Cereda, D.R. de Araujo, E. de Paula, R.B. Brito Jr., J. Pedrazzoli Jr., E. Meurer, F.A. Barros, F.C. Groppo, M.C. Volpato, J. Ranali, Pharmacokinetic and local toxicity studies of liposome-encapsulated and plain mepivacaine solutions in rats, Drug Deliv. 17 (2010) 68–76.
[38] J.N. Francischi, C.T. Chaves, A.C. Moura, A.S. Lima, O.A. Rocha, D.L. Ferreira-Alves, Y.S. Bakhle, Selective inhibitors of cyclooxygenase-2 (COX-2) induce hypoalgesia in a rat paw model of inflammation, Br. J. Pharmacol. 137 (2002) 837–844.
[39] Z. Pourpak, A. Ahmadiani, M. Alebouyeh, Involvement of interleukin-1beta in systemic morphine effects on paw oedema in a mouse model of acute inflammation, Scand. J. Immunol. 59 (2004) 273–277.
[40] E. de Paula, C.M. Cereda, L.F. Fraceto, D.R. de Araujo, M. Franz-Montan, G.R. Tofoli, J. Ranali, M.C. Volpato, F.C. Groppo, Micro and nanosystems for delivering local anesthetics, Expert Opin. Drug. Deliv. 9 (2012) 1505–1524.
[41] K.R. Bagshaw, C.L. Hanenbaum, E.J. Carbone, K.W. Lo, C.T. Laurencin, J. Walker, L.S. Nair, Pain management via local anesthetics and responsive hydrogels, Ther. Deliv. 6 (2015) 165–176.
[42] D. Seol, M.J. Magnetta, P.S. Ramakrishnan, G.L. Kurriger, H. Choe, K. Jang, J.A. Martin, T.H. Lim, Biocompatibility and preclinical feasibility tests of a temperature-sensitive hydrogel for the purpose of surgical wound pain control and cartilage repair, J. Biomed. Mater. Res. B Appl. Biomater. 101 (2013) 1508–1515.
[43] F. Taraballi, S. Minardi, B. Corradetti, I.K. Yazdi, M.A. Balliano, J.L. Van Eps, M. Allegri, E. Tasciotti, Potential avoidance of adverse analgesic effects using a biologically "smart" hydrogel capable of controlled bupivacaine release, J. Pharm. Sci. 103 (2014) 3724–3732.
[44] P.L. Foley, B.D. Ulery, H.M. Kan, M.V. Burks, Z. Cui, Q. Wu, L.S. Nair, C.T. Laurencin, A chitosan thermogel for delivery of ropivacaine in regional musculoskeletal anesthesia, Biomaterials 34 (2013) 2539–2546.